Proceedings of
ASME TURBO EXPO 2002
June 3-6, 2002, Amsterdam, The Netherlands

GT-2002-30552

FILM COOLING: A COMPARATIVE STUDY OF DIFFERENT HEATER-FOILCONFIGURATIONS FOR LIQUID CRYSTALS EXPERIMENTS

G. Vogel and A. Graf
Laboratoire de Thermique Appliquée et de Turbomachines (LTT)
Swiss Federal Institute of Technology
CH-1015 Lausanne, Switzerland

B. Weigand
Institute for Aerospace Thermodynamics (ITLR)
University of Stuttgart
D-70569 Stuttgart, Germany

ABSTRACT

A new measurement technique for the determination of the heat transfer coefficient and the film cooling effectiveness is presented. It is based on a regression of multiple transient liquid crystals experiments using an electrical heater-foil producing a non-homogeneous surface heat flux. This is particularly interesting for film-cooled surfaces where each cooling hole in the heater-foil leads to a non-homogeneous heat flux distribution. The method and its theoretical basis are described. Results on two different heater-foil configurations for one row of film cooling holes are presented. The first heater-foil configuration deals with a longitudinal electrical current relatively to the main flow direction, while the second one is considering a transversal electrical current.

NOMENCLATURE

BR [-]	blowing ratio
c_p [J/(kgK)]	specific heat at constant pressure
d [m]	film cooling hole diameter
G [-]	gain factor
h [W/(m^{2}K)]	convective heat transfer coefficient
k [W/mK]	thermal conductivity
L [m]	wall thickness
N [-]	number of experiments
P [m]	pitch cooling holes
q [W/m^2]	surface reference heat flux
T [K]	temperature
t [s]	time
x [m]	spatial coordinate into the material
y,z [m]	surface coordinates on the plate

GREEK

α [m^2/s]	thermal diffusivity $\alpha=k/(\rho c_p)$
η [-]	film cooling effectiveness
ρ [kg/m^3]	density

SUBSCRIPTS

0	initial condition (t=0)
aw	adiabatic wall
i	index of experiment
LC	liquid crystal
rg	recovery gas
tg	total gas
tc	total coolant
w	wall (x=0)

INTRODUCTION

In modern gas turbine design, there is a strong desire to increase the inlet hot-gas temperature of the turbine. This would lead to much higher blade temperatures than the maximum allowable metal temperature of the gas turbine blades. In order to protect the turbine blades from melting, the blades need extensive cooling by internal air flow. Usually a combination of internal convective cooling and external film cooling is employed. The cooling designs of these parts have to be highly efficient, because a larger cooling mass flow rate degrades the thermal efficiency of the thermodynamic cycle of the gas turbine. This is especially true for the application of film cooling, where a protective film of cold air is spread around the blade and large cooling mass flows are required. Because of the importance of film cooling for turbine blade design, the subject has been studied

extensively over the past 35 years [1-3]. Most of the studies concentrate on flat plate configurations with film injection through slots, cylindrical or shaped holes [4,5]. When film cooling is considered on airfoil type flows [6-8], numerical methods and correlations have been developed to predict the adiabatic film cooling effectiveness and the increase in heat transfer coefficients, a large number of parameters influencing the film cooling process (such as cooling hole geometry, blowing and momentum flux ratio and main stream turbulence effects). Several models can be found in literature and are used for specific applications only [9-11]. In order to further develop the cooling schemes for gas turbine blades, high quality experimental data are required. Today, in order to obtain these data, a large number of heat transfer experiments are performed by using the liquid crystals technique. Herewith, it is possible to obtain the film cooling performance (adiabatic film cooling effectiveness and increase in film cooling heat transfer coefficients) either by two separate experiments, or by transient experiments.

If two separate experiments are performed, the increase in heat transfer coefficient is measured by using the steady-state liquid crystals method for a film cooling injection experiment, where the coolant temperature and the free stream temperature are identical. The increase in heat transfer due to film cooling is obtained by applying a heater-foil at the wall. The adiabatic film cooling effectiveness is additionally measured by using an adiabatic wall and by blowing with a different coolant temperature than the main stream temperature [12].

Using the transient liquid crystals approach, film cooling performance can be obtained by varying the coolant temperature for several runs and employing a regression analysis. These transient experiments are generally performed by the rapid insertion of a preconditioned model [13,14] or by using heater grids in the main flow.

Because of the demand to obtain high quality experimental data, new liquid crystals measurement techniques have been developed. One is given in [15] where a step heating technique is described for heat transfer measurements without film cooling. The method has the advantage that uncertainties and losses in the power for the heater-foil do not influence the measured heat transfer coefficient.

The objective of the present paper is to introduce a new transient heater-foil method for film cooling situations. By using this new method, the film cooling effectiveness and the heat transfer augmentation can be obtained simultaneously. An analytical theory of this new method is developed. Experimental results on a flat plate with cylindrical film cooling holes are shown for two heater-foil configurations. Results are compared to a correlation issued from experimental data given in the literature.

MEASUREMENT TECHNIQUE: THEORY

Consideration is given to a flat plate geometry covered by a heater-foil having a row of film cooling holes. The flat plate is subjected to a longitudinal main flow. A transient measurement technique as shown in Fig 1 is developed: at t_0=0, a step change in the surface heat flux $q(t)$ is generated by the heater-foil and at the same time a coolant gas is injected at a constant blowing ratio but with a temperature evolution $T_{tc}(t)$.

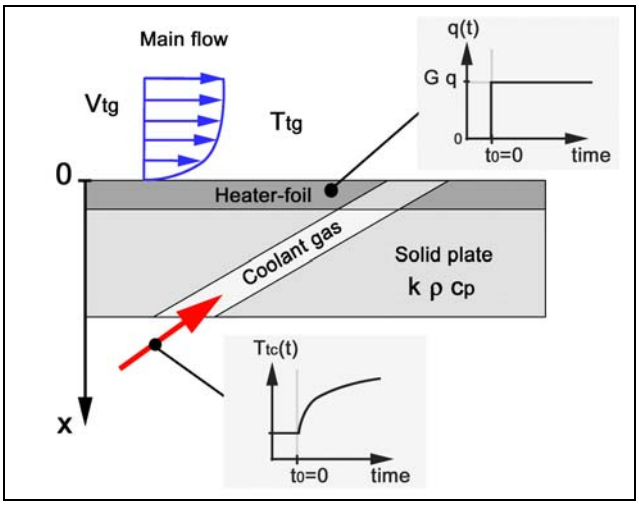

Fig 1: Schematic drawing of the considered flat plate experiment.

The equation describing the spatio-temporal evolution of the temperature at a specific location in the plate is given by the one-dimensional heat conduction equation without source terms:

$$\frac{\partial T(x,t)}{\partial t} = \alpha \frac{\partial^2 T(x,t)}{\partial x^2} \tag{1}$$

The initial condition is written as:

$$T(x,0) = T_0 \tag{2}$$

It can be shown [16] that if the transient time of the experiment is shorter than a certain value, the plate can be considered as semi-infinite in the x direction, yielding:

$$t < \frac{L^2}{4\alpha} \quad \Rightarrow \quad T(\infty,t) = T_0 \tag{3}$$

Assuming the heater-foil infinitely thin compared to the thickness of the plate, conservation of energy implies that the conductive and convective heat flux on the surface (Eq.(5) and Eq.(6) respectively) are equal to the surface heat flux generated by the foil $q(t)$ as:

$$q(t) = q_{conduction}(t) + q_{convection}(t) \tag{4}$$

where

$$q_{conduction}(t) = -k \frac{\partial T(0,t)}{\partial x} \tag{5}$$

$$q_{convection}(t) = -h(T_{aw}(t) - T(0,t)) \tag{6}$$

and T_{aw} being expressed by the film cooling effectiveness defined as:

$$\eta = \frac{T_{aw}(t) - T_{rg}}{T_{tc}(t) - T_{tg}} \tag{7}$$

Eqs.(4)-(7) imply:

$$q(t) = -k\frac{\partial T(0,t)}{\partial x} + h(T(0,t)) - T_{rg}) + \eta\, h(T_{tg} - T_{tc}(t)) \qquad (8)$$

For the transient experiments described above, the heat flux and the cooling temperature vary as follows:

$$\begin{cases} q(t \le 0) = 0 \\ q(t > 0) = G\, q \end{cases} \quad (9) \qquad \text{and} \qquad T_{tc}(t) = a\, e^{bt} + c\, t + d\sqrt{t} \quad (10)$$

where G stands for a gain with respect to a "reference" heat flux q, and a,b,c,d are constants fitting the experimental profile of $T_{tc}(t)$. The analytical solution for the heat conduction equation under the previous assumptions can be carried out by using the Laplace transform, yielding the surface (x=0) temperature evolution on the flat plate as:

$$T_w(h,\eta,q) = A(h) + \eta\, B(h) + q\, C(h) \qquad (11)$$

where for b>0:

$$A(h) = T_0 + \left(T_{rg} - T_0\right)\left[1 - e^{\beta^2}\, erfc(\beta)\right]$$

$$B(h) = -T_{tg}\left[1 - e^{\beta^2}\, erfc(\beta)\right] + \\ + \frac{h}{k}\left[\frac{a\cdot e^{b\cdot t}}{2}\left\{\frac{\sqrt{\alpha}}{\frac{h}{k}\sqrt{\alpha}+\sqrt{b}}\, erfc\left(-\sqrt{b\cdot t}\right) + \frac{\sqrt{\alpha}}{\frac{h}{k}\sqrt{\alpha}-\sqrt{b}}\, erfc\left(\sqrt{b\cdot t}\right)\right\} - \frac{\alpha a}{\frac{h}{k}\alpha - \frac{kb}{h}}\, e^{\beta^2}\, erfc(\beta)\right] - \\ - \frac{h}{k}\left[\frac{c}{\alpha\left(\frac{h}{k}\right)^3}\left(e^{\beta^2}\, erfc(\beta) - \sum_{r=0}^{2}\frac{(-\beta)^r}{\Gamma\left(\frac{r}{2}+1\right)}\right)\right] + \\ + \frac{h}{k}\left[\frac{d\sqrt{\pi}}{2\sqrt{\alpha}\left(\frac{h}{k}\right)^2}\left(e^{\beta^2}\, erfc(\beta) - \sum_{r=0}^{1}\frac{(-\beta)^r}{\Gamma\left(\frac{r}{2}+1\right)}\right)\right]$$

$$C(h) = \frac{G}{h}\left[1 - e^{\beta^2}\, erfc(\beta)\right]$$

and $\beta^2 = \left(\frac{h}{k}\right)^2 \alpha\, t$

Γ the gamma function and *erfc* the complementary error function. When b<0 the term of $B(h)$ in {} is expressed as follows:

$$\left\{\frac{\sqrt{\alpha}}{\frac{h}{k}\sqrt{\alpha}+\sqrt{b}}\, erfc\left(-\sqrt{bt}\right) + \frac{\sqrt{\alpha}}{\frac{h}{k}\sqrt{\alpha}-\sqrt{b}}\, erfc\left(\sqrt{bt}\right)\right\} = \left\{\frac{2\sqrt{\alpha}}{\left(\frac{h}{k}\right)^2\alpha + b}\left(\frac{h}{k}\sqrt{\alpha} + 2\sqrt{\frac{-b}{\pi}}\left(\int_0^{\sqrt{-bt}} e^{t^2}\, dt\right)\right)\right\}$$

For the case of a constant heat flux generated by a heater-foil and when there is no film cooling (η=0), Eq.(11) reduces to the expression given in [15].

REGRESSION

For the transient experiment considered in this paper, the parameters to be determined are h and η. Moreover since the surface heat flux is not measurable, the method proposed here considers q as an unknown, and thus also determines it. The determination of h, η and q is done using a one-dimensional non-linear least-square regression.

By applying a coating of narrow-band liquid crystals on the surface of the plate, it is possible to obtain for any position *(y,z)* on the plate the time t_{LC} at which a specific temperature T_{LC} appears during a transient experiment as:

$$T_w(h,\eta,q)\big|_{t=t_{LC}} = T_{LC} \qquad (12)$$

The values of t_{LC} for one specific transient experiment vary locally on the surface as they depend on the heat transfer coefficient h, the film cooling effectiveness η and the heat flux q since the latter will vary non-homogenously over the presence of the cooling holes (and for a possible thickness change of the foil). Hence, by using the transient liquid crystals technique allowing to determine T_{LC} and t_{LC}, by measuring the parameters T_{tg}, T_{rg}, T_0, $T_{tc}(t)$, G and by knowing the properties of the material, the unknowns left in Eq.(11) are h, η and q. By performing at least three independent experiments it is then possible by the use of a non-linear least-squares regression [8] to determine these unknowns.

Assuming for each experiment i, as given by Eq.(12):

$$T_w(h,\eta,q)\big|_{t=t_{LCi}} - T_{LCi} = 0 \quad \forall i = 1,...,N \qquad (13)$$

for $N \geq 3$, the optimal solution for the three unknowns parameters which fits best these N equations (without necessarily satisfying them all exactly) is then given by the minimum of the following error function:

$$\sum_{i=1}^{N}\left[T_w(h,\eta,q)\big|_{t=t_{LCi}} - T_{LCi}\right]^2 = e(h,\eta,q) \geq 0 \qquad (14)$$

By considering each experiment as one component of a vector, Eq.(11) can be written in vector form as follow:

$$\vec{T}_w(h,\eta,q) = \vec{A}(h) + \eta\vec{B}(h) + q\vec{C}(h) \qquad (15)$$

Thus the following error function is obtained:

$$e(h,\eta,q) = \frac{1}{2}\left\|\vec{T}_w(h,\eta,q) - \vec{T}_{LC}\right\|^2 = \frac{1}{2}\left\|\vec{A}(h) + \eta\vec{B}(h) + q\vec{C}(h) - \vec{T}_{LC}\right\|^2 \qquad (16)$$

This error is minimum when:

$$\vec{\nabla} e(h,\eta,q) = 0 \quad \Rightarrow \quad \frac{\partial e}{\partial \eta} = 0 \quad \frac{\partial e}{\partial q} = 0 \quad \frac{\partial e}{\partial h} = 0 \qquad (17)$$

By using Eq.(17) it is possible to express η as a function of h and q:

$$\frac{\partial e}{\partial \eta} = 0 \quad \Rightarrow \quad \eta(h,q) = \frac{\left(\vec{T}_{LC} - q\,\vec{C}(h) - \vec{A}(h)\right)\cdot\vec{B}(h)}{\left\|\vec{B}(h)\right\|^2} \qquad (18)$$

and q as function of h:

$$\frac{\partial e}{\partial q} = 0 \quad \Rightarrow \quad q(h) = \frac{\left(\vec{T}_{LC} - \vec{A}(h) - \frac{\left(\vec{T}_{LC} - \vec{A}(h)\right)\cdot\vec{B}(h)}{\left\|\vec{B}(h)\right\|^2}\vec{B}(h)\right)\cdot\vec{\omega}(h)}{\left\|\vec{\omega}(h)\right\|^2} \qquad (19)$$

where: $\vec{\omega}(h) = \vec{C}(h) - \dfrac{\vec{C}(h)\cdot\vec{B}(h)}{\left\|\vec{B}(h)\right\|^2}\vec{B}(h)$

Inserting Eqs.(18)-(19) into Eq.(16) yields an error function which is only dependant upon h. The three-parameter optimization problem is hence reduced to a one-dimensional one, which can easily be solved. The optimum of h is first obtained, then the corresponding optimum q and finally the optimum η are computed.

EXPERIMENTAL SETUP:
TEST FACILITY

Experiments have been carried out in an open low speed wind tunnel as represented in Fig 2. The air flow is generated by two fans mounted in series followed by a settling chamber and a convergent nozzle. The channel at the exit of the nozzle has a squared cross-section of 100 mm x 100 mm and a total length of 1500 mm. In order to have good optical access and low thermal conductivity, the walls of the channel were made out of Perspex.

The flat plate test section of L=25 mm thickness and 250 mm length covering the width of the channel (100 mm) was mounted into the lower wall of the channel at 10 hydraulic diameters from the inlet. Introducing a small step at the start of the test section guaranteed a turbulent boundary layer. The test section is film-cooled by a row of five cylindrical holes, having an exit angle of 30° to the surface. The holes have a diameter of d=5 mm and the ratio between the length of the hole L_d to the diameter is L_d/d>3. The five holes are centered in the transversal (spanwise) direction of the channel with a pitch of P/d=3.5. The row in the longitudinal (streamwise) direction is located at 30 hole diameters after the start of the plate as shown in Fig 6.

The plenum chamber for the coolant flow injection is mounted on the lower part of the test section. The coolant blowing ratio is adjusted by measuring the mass flow given by a graduated glass flow meter. The temperature of the coolant flow can be varied by an electrical heater tube, a by-pass vane allowing the preconditioning of the flow before the transient test. A thermocouple inserted in the plenum chamber measures the coolant flow temperature during the experiment.

The heater-foil of 20 μm thick nickel-chrome material is glued onto the surface. The foil has been connected to a power supply device through copper cables and bus bars mounted laterally to the plate for one test configuration and longitudinally to the plate for another test configuration (see Fig 6). Thermocouples mounted slightly under the upper surface of the plate (for electrical insulation) were used to measure the initial surface temperature. Monitoring of thermocouples positioned on the lower plate surface allowed to verify the semi-infinite model assumption.

A black coating layer followed by a thermo-chromic narrow band liquid crystals layer is applied on the test section. A thermocouple mounted on top of these layers is used for the hue-temperature calibration. Hue value variations on the surface are recorded during the transient experiment by a 25 Hz color CCD camera mounted perpendicular to the flat plate. The time t_{LC} are obtained by performing a data reduction of the hue signal [17]. Cold light sources are used for the illumination of the test section. A red LED triggered by the power supply is placed on the recorded area, outside of the channel on the lateral wall, in order to determine the beginning of the transient experiment on the video sequences. The trigger coming from the power supply signal is also used for the synchronization of the coolant flow injection and the step surface heat flux generation.

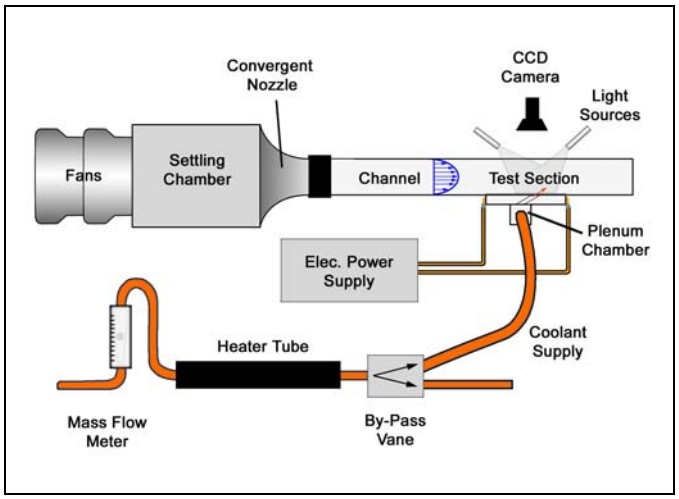

Fig 2: Schematic drawing of the test facility.

TEST CASES

Transient experiments have been performed for an exit flow velocity of ~22 m/s at a total gas temperature of ~23°C. Initial temperatures were in the same range and a specific hue value of the narrow band liquid crystals was calibrated at 36.2 °C. The film cooling blowing ratio was set to BR=0.3 and the coolant gas temperature evolution varied from 27°C to 33°C for N transient experiments. The variable amount of heat flux applied during the experiments was chosen in order to have a time event detection neither too short (t_{LC}>2 s) because of the rapid evolution of T_w at the beginning of the transient test, nor too long (t_{LC} <1200 s) in order to respect the semi-infinite model assumption.

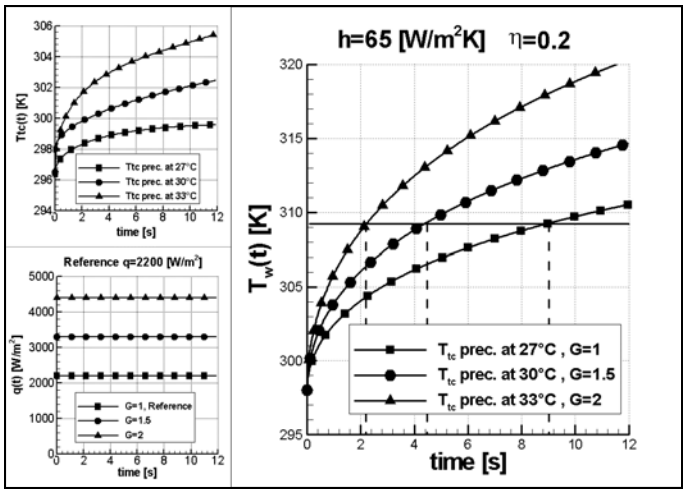

Fig 3: Numerical predictions of T_w(t) for Ttc(t) and q(t).

Numerical simulations of the temporal evolution of T_w were performed in order to predict a guess for the values of t_{LC}. The right hand-side graph in Fig 3 represents the wall temperature profiles, for h=65 W/m^{2}K, η=0.2, for three different coolant temperature

evolutions $T_{tc}(t)$ and three heat flux gains G_i with a reference heat flux of q=2200 W/m^2. The upper left hand-side graph in Fig 3 represents the three $T_{tc}(t)$ used. Their temperature profiles are representative from the experiments where the coolant flow is first preconditioned at a certain temperature level and then injected into the plenum chamber. For the sake of graphical representation, the preconditioned coolant temperature and the gain factor of this simulation are varied simultaneously, although it is also possible to apply different G_i for the same $T_{tc}(t)$. The G_i used here are shown on the lower left hand-side graph in Fig 3. Finally, the predicted values of t_{LC} of each case are given by the intersection of T_{LC} in the right hand-side graph in Fig 3 (dashed vertical lines).

For each experiment, typically a total of nine tests (N=9) were measured, consisting of all the combinations of three different heat flux ratios with three different coolant temperature preconditionings.

Experiments have been performed on two different heater-foil configurations, as shown in Fig 6:

Case 1: Bus bars perpendicular to the flow direction forcing a global longitudinal electrical current in the foil.

Case 2: Bus bars parallel to the flow direction forcing a global transversal electrical current in the foil.

In both cases non-homogeneities of the local heat flux generated by the foil existed because of the presence of the cooling holes on the foil. The fact that the electrical current was different between both cases also generated a different heat flux distribution. Since the measurement technique described in this paper is developed for heater-foil experiments with an unknown surface heat flux distribution q, the two different cases described above provide a good illustration of its usefulness and general applicability.

MEASUREMENT ERRORS

Errors on the heat transfer coefficient and the film cooling effectiveness appear to be higher near the holes where the surface heat flux has extreme local values. Moreover the semi-infinite model assumption is not satisfied there anymore. Faster transient experiments lead to higher errors due to a limited time resolution for t_{LC}. The temperature levels used for the transient experiments have to be chosen in accordance with the precision on the temperature measurements. Hence for the experiments done in this paper, the error analysis based on an absolute t_{LC} error of 0.04 s and an absolute temperature error of 0.1°C on each temperature variable, yields an average relative error of ~5% on h, of ~6% on η and of ~2% on q (for nominal values of h, η and q as presented in Fig 3.)

RESULTS AND DISCUSSION:

Some preliminary experiments have first been performed on a simpler configuration without holes in the heater-foil (hence homogeneous heat flux and no film cooling η=0). The goal was to verify the baseline heat transfer values h_0 for the chosen flow conditions as well as obtaining a homogeneous heat flux distribution q_0. The results given below are then presented in dimensionless form by the use of these reference values. Note that these baseline reference values are identical for either a longitudinal or transversal electrical current directions as the heat flux is homogeneous for a heater foil without the presence of the holes.

For each of the two foils configurations, the nine different transient experiments performed were run with the same three different coolant temperature preconditionings. The surface reference heat flux q and the gain values G_i were chosen so that the total duration of the different sets of transient experiments were about the same for the two cases, the experiment being considered as finished when the liquid crystals signal was detected all over the surface. The lowest heat flux case was considered as the reference q, hence corresponding to a gain G_i=1.

HEAT FLUX

The reference heat flux q obtained by the regression is presented in its non-dimensional form q/q_0 in Fig 7. The effective surface heat flux generation applied during each experiment i is then the product of q by its gain factor G_i.

For case 1, the local surface heat flux tends to increase in-between the holes and decreases in the longitudinal prolongation of the holes. The opposite is true for case 2 where the local surface heat flux is low or close to zero in-between the holes (resulting in a white zone area as no transient liquid crystal signal was detected) and increases in their longitudinal prolongations The heat flux values on the regions upstream and downstream attached to the shape of holes are very high. The transient liquid crystal signal is hence difficult to acquire in this area resulting in white bubbles areas on case 2 of Fig 7. This corresponds to the expected result when considering the local surface resistance of the foil and the path of the electrical current.

The surface heat flux distributions in these two cases have been compared to numerical simulations done using a method described in [18]. The calculated values are superposed to the color values of the measurements in the graph (see Fig 7). They show excellent agreement and hence validate the regression approach of multiple transient heater-foil experiments and the development of the new measurement technique described above regarding the heat flux determination. Notice that with this novel measurement technique, the heat flux losses (electrical wiring, lateral conduction) are automatically accounted for without explicit knowledge of them. Furthermore these losses were determined by assessing the difference between the power given by the power supply and the surface heat power q yielding a difference of ~25%.

Depending on the optical access and light setup, the time detection extracted from the liquid crystals video sequences can in some cases produce noise on the results, like the small dots for case 1 on the right hand-side of the row of film cooling holes. The dot on case 2 on the left hand-side of the row is however due to the presence of an undesired glue bubble that appeared while the foil was applied on the surface.

HEAT TRANSFER COEFFICIENT

The two upper graphs of Fig 8 show the distribution of the heat transfer coefficient for both heater-foil configurations. Both cases show a slight increase of h behind the cooling holes, which is a consequence of the increase in turbulence due to the cooling flow injection.

In order to compare the experimental values of h, a transversal averaging over one hole pitch length around the center hole for each downstream longitudinal coordinate (see black rectangles in Fig 8) was performed as presented in Fig 4. Despite the absolute value of h being relatively low for this experiment and hence with a some uncertainties, values of the two cases are relatively close to each other which shows that the two different heater-foil configurations result only in small changes of the heat transfer coefficient. Only values of $z/d<1$ have to be considered are there is some uncertainties just around the hole exit. Additionally, because of the low blowing rate, no significant increase in heat transfer coefficients can be observed.

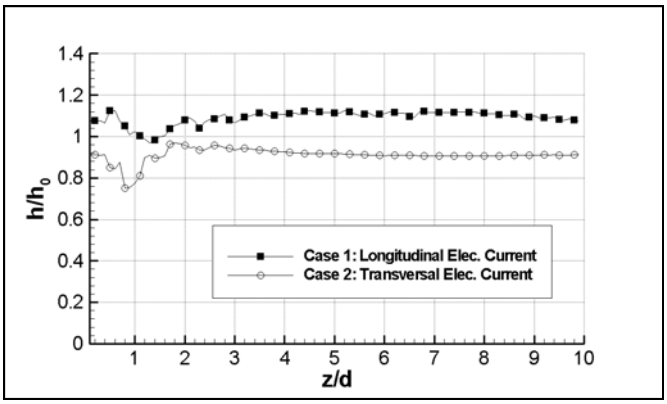

Fig 4: Dimensionless averaged *h* over one hole pitch.

FILM COOLING EFFECTIVENESS

The two lower graphs of Fig 8 show the film cooling effectiveness for the two heater-foil configurations. Both cases show as expected an increase of η behind the cooling holes. It can be noted that this effect is not perfectly periodic over the hole pitch since there is a small gradient in the transversal direction. This occurs for both cases and can be the consequence of the presence of a pressure gradient in the plenum chamber due to a lateral feeding of the coolant flow.

Results of the transversal case close to the downstream border of the foil (z/d>10) have been influenced by a lack of t_{LC} signal detection during the multiple test experiments. From the two figures it can be concluded that there is also only a small effect of the two chosen heater-foil configurations on the values of the adiabatic film cooling effectiveness.

In order to compare the obtained values of η, an identical transversal averaging as described above yields the curves presented in Fig 5. Moreover the results of a correlation as given in [19] are also presented, this correlation being based on a large set of experimental data. As it can be noticed, the three curves exhibit a similar behavior, the reason for the slight disagreement in the near hole area being due to measurements uncertainties in the regions of extreme values of the surface heat flux. Moreover the experimental curves being close to the correlation curve, the measurement technique introduced in this paper is hence validated.

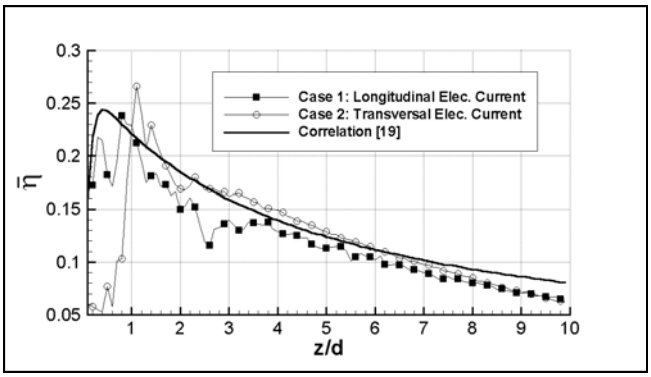

Fig 5: Dimensionless averaged η over one hole pitch.

CONCLUSIONS

In this paper, a novel method for determining the heat transfer coefficient and film cooling effectiveness is presented. This method is based on the liquid crystals technique applied on a heater-foil with film cooling holes. Two heater-foil configurations were considered. The measurements obtained in these two cases, both with heavily non-homogeneous surface heat fluxes, gave the same heat transfer coefficient level and film cooling effectiveness distributions, thus corroborating the theoretical developments. Moreover the values obtained showed good agreement with data given in literature. This new measurement technique also allowed to determine the surface heat flux distribution, the latter having successfully been compared to numerical simulations. The above results validated the regression approach of multiple liquid crystals transient heater-foil experiments for the determination of the heat transfer coefficient, the film cooling effectiveness and the surface heat-flux.

This novel method allows transient measurements for complex film cooled surfaces such as platforms where it is not possible to have a heater foil with homogeneous heat flux. Since the heat flux is determined, it also eliminates the process of estimating the heat losses. Further investigations will include the study of other heater-foil configurations and a more detailed error analysis.

ACKNOWLEDGEMENT

The authors acknowledge the help of Prof. J. von Wolfersdorf for carrying out the numerical simulations of the surface heat flux in the two heater-foil configurations.

REFERENCES

1. Goldstein, R.J., 1971, "Film Cooling. In Advances in Heat Transfer", Irvine T.F. and J.P. Hartnett Eds. Academic Press, New York, **7**, pp. 321-379.
2. VKI Lecture Series, 1982, "Film Cooling and Turbine Blade Heat Transfer", VKI-LS 82-02.
3. Leontiev, A.I., 1999, "Heat and Mass Transfer Problems for Film Cooling", Journal of Heat Transfer, **121**, pp. 509-527.
4. Sinha, A.K, Bogard, D.G. & M.E. Crawford, 1990, "Film Cooling Effectiveness Downstream of a Single Row of Holes with Variable Density Ratio", 90-GT-43.
5. Forth, C.J., Loftus, P.J. & T.V. Jones, 1980, "The Effect of Density Ratio on the Film Cooling of a Flat Plate", AGARD CP 390, Bergen.
6. Ito, S., Goldstein, R.J. & E.R.G. Eckert, 1978. "Film Cooling of a Gas Turbine Blade", J. Eng. for Power, **100**, pp. 476-481.
7. Takeishi, K., Aoki, S., Sato, T. & K. Tsukagoshi, 1992, "Film Cooling on a Gas Turbine Rotor Blade", J. of Turbomachinery, **114**, pp. 828 – 834.
8. Drost, U., 1998, "An Experimental Investigation of Gas Turbine Airfoil Aero-Thermal Film Cooling Performance", Thesis N°1817, EPF Lausanne, Switzerland.
9. Crawford, M.E., 1986, "Simulation codes for calculation of heat transfer to convectively cooled turbine blades", VKI-LS, Convective heat transfer and film cooling in turbomachinery.
10. Weigand, B., Bonhoff, B. & J. Ferguson, 1997, "A comparative study between 2D boundary layer predictions and 3D Navier-Stokes calculations for a film cooled vane", National Heat Transfer Conference, Batimore, HTD 350, pp. 213-221.
11. Garg, V.K., 1997, "Comparison of Predicted and Experimental Heat Transfer on a Film-Cooled Rotating Blade using a Two-Equation Turbulence Model", 97-GT-220.

12. Lutum, E., von Wolfersdorf, J., Weigand, B.& K. Semmler, 2000, “Film Cooling on a convex surface with zero pressure gradient flow”, Int. J. Heat Mass Transfer, **43**, pp. 2973-2987.
13. Reiss, H. et al. 1998, “The Transient Liquid Crystal Technique Employed for Sub- and Transonic Heat Transfer and Film Cooling Measurements in a Linear Cascade”, 14th bi-annual symposium on Measurement Techniques in Transonic and Supersonic Flow in Cascades and Turbomachines.
14. Dui, H., J.C., Han & Ekkad, V., 1997, “Detailed film cooling measurements over a gas turbine blade using a transient liquid crystal image technique”, HTD 350, National Heat Transfer Conference, **12**.
15. Von Wolfersdorf, J., Hoecker, R., Sattelmayer, T., 1992, “A hybrid Transient Step-Heating Heat Transfer Measurement Technique Using Heater Foils and Liquid-Crystal Thermography”, Journal of Heat Transfer, **115**, pp. 319-324.
16. Vogel, G. and Weigand, B., 2001, “A New Evaluation Method for Transient Liquid Crystal Experiments”, NHTC01-1511, 35th ASME National Heat Transfer Conference, Anaheim, USA.
17. Vogel, G. and Bölcs, A., 2000, “A Novel Digital Image Processing System for the Transient Liquid Crystal Technique applied for Heat transfer and Film Cooling Measurements”, ICHMT Paper, Turbine-2000 Symposium, Cesme, Turkey.
18. Wiedner, B.G. and Camci, C., 1996, “Determination of Convective Heat Flux on Steady-State Heat Transfer Surface With Arbitrarily Specified Boundaries”, Journal of Heat Transfer, **118**, pp. 850-856.
19. Baldauf, S., Schulz, A., Wittig, S. and Schleurlen, M., 1997, “An Overall Correlation of Film Cooling Effectiveness from One Row of Holes”, 97-GT-79.

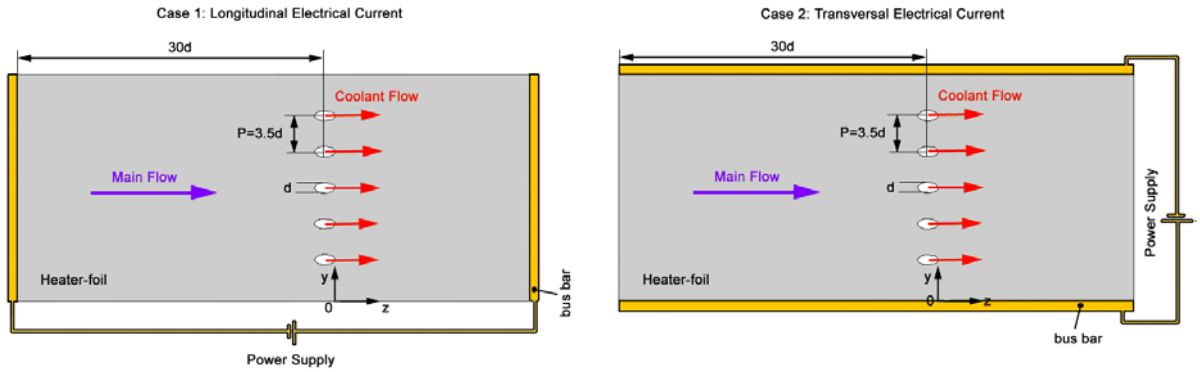

Fig 6: Heater-foil configurations of the 2 test cases.

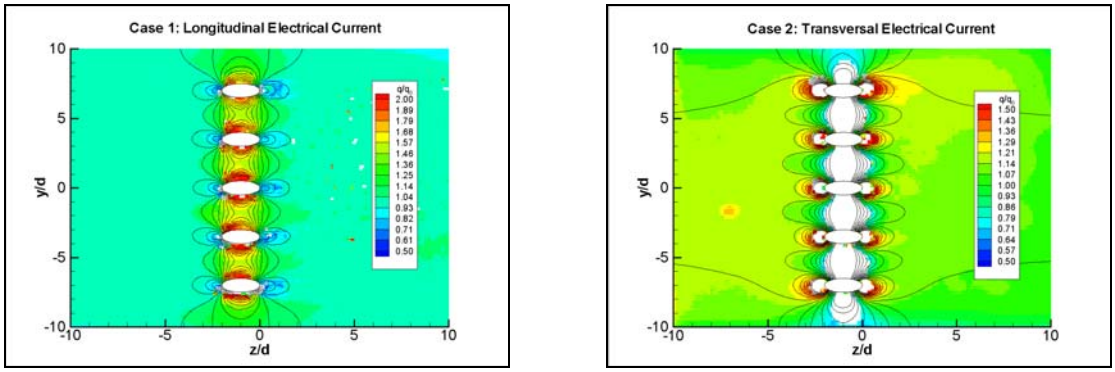

Fig 7: Dimensionless reference heat flux distributions, measurements (colors) and simulations (lines) for the 2 test cases.

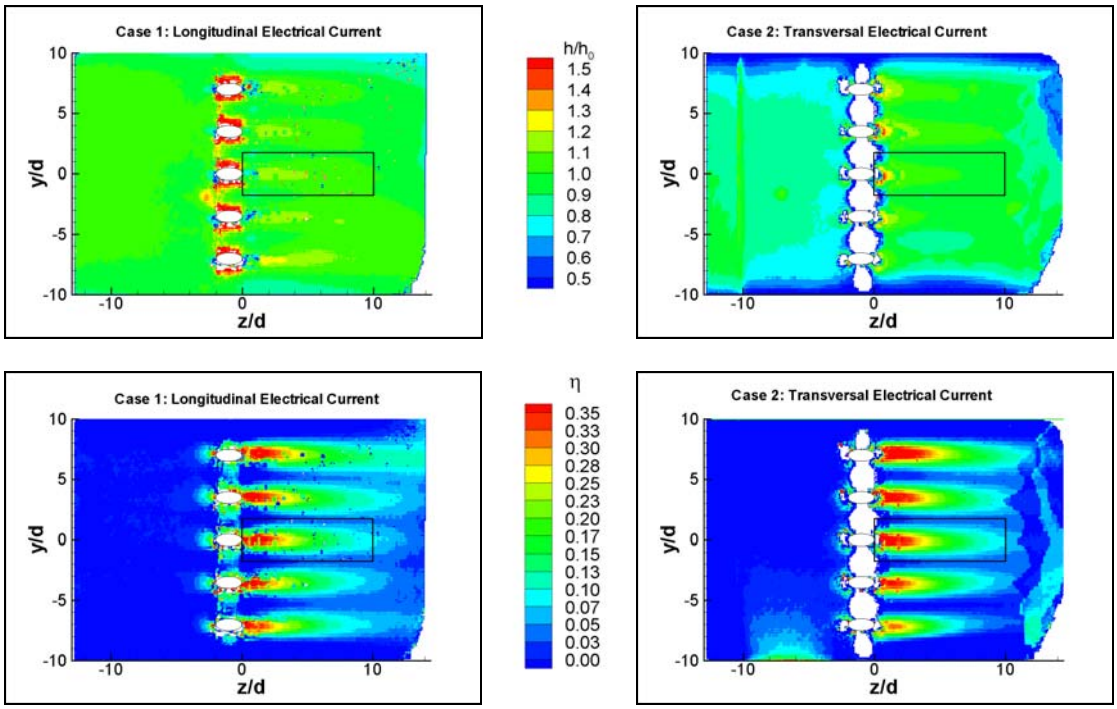

Fig 8: Dimensionless heat transfer coefficient and film cooling effectiveness distributions for the 2 test cases.